Royal Society Publishing

Testing the optimality properties of a dual antibiotic treatment in a two-locus, two-allele model

Rafael Peña-Miller[1], Ayari Fuentes-Hernandez[1], Carlos Reding[2], Ivana Gudelj[2] and Robert Beardmore[2]

[1]Centro de Ciencias Genómicas, Universidad Nacional Autónoma de México, Cuernavaca, Morelos, México
[2]Department of Biosciences, University of Exeter, Exeter EX4 4SB, UK

Mathematically speaking, it is self-evident that the optimal control of complex, dynamical systems with many interacting components cannot be achieved with 'non-responsive' control strategies that are constant through time. Although there are notable exceptions, this is usually how we design treatments with antimicrobial drugs when we give the same dose and the same antibiotic combination each day. Here, we use a frequency- and density-dependent pharmacogenetics mathematical model based on a standard, two-locus, two-allele representation of how bacteria resist antibiotics to probe the question of whether optimal antibiotic treatments might, in fact, be constant through time. The model describes the ecological and evolutionary dynamics of different sub-populations of the bacterium *Escherichia coli* that compete for a single limiting resource in a two-drug environment. We use *in vitro* evolutionary experiments to calibrate and test the model and show that antibiotic environments can support dynamically changing and heterogeneous population structures. We then demonstrate, theoretically and empirically, that the best treatment strategies should adapt through time and constant strategies are not optimal.

1. Introduction

The discovery of antibiotics provided medics with a tool of unprecedented potency in the battle against bacterial pathogens [1]. However, we are now engaged in an arms race where bacteria seem to be, at least for the moment, firmly in the ascendancy and new ideas for deploying antibiotics are needed. Bacteria have evolved resistance to every antibiotic in clinical use [2], and the correlation between drug usage and resistance evolution [3] suggests our attitudes towards antimicrobials are, at least in part, responsible for our problems. Antibiotics have been misused [4] and overprescribed [5], and problems in the economic model due to resistance have lead the pharmaceutical industry to abandon their antimicrobial discovery programmes [6,7].

However, simply finding more antibiotic small molecules will not provide a sustainable solution to these issues. The timeline from antibiotic discovery to drug-resistant clinical isolate is of the order of a decade, or two [3], so unless we have a library of drug usage protocols successful both at clearing bacterial infections and at preserving their efficacy, any novel antimicrobial substance would be predestined to eventual failure.

Finding long-lasting solutions to antibiotic resistance is an exceptionally difficult problem, well-beyond the scope of a theoretical study such as this, but we contend that theoretical frameworks exploiting the theory of dynamical systems, control and optimization might be developed that provide insight and contribute much to the design of rational drug deployment strategies.

With this in mind, we ask the question: what if treatment fails to achieve inhibitory doses everywhere at all times and resistance develops? What principles might there then be behind optimal dosing strategies? Seeking answers, we pose a pharmacogenetics theoretical model of an experimental microcosm (with

parameter values calibrated using *in vitro* experimental data) and use it to illustrate a very simple control engineering principle: the optimal treatment is contingent upon treatment duration and, as a result, the treatment may need to be adapted through time.

1.1. Optimal antibiotic treatments

An optimal antibiotic deployment strategy is often seen as having two features to reconcile: (i) the dose and (ii) the duration of treatment, both are a matter of some controversy.

First, there is no consensus on the optimal length of treatment. It has been reported that the number of pills per patient favours odd over even numbers, the reason behind this statistical anomaly is an unwritten rule, whereby treatment duration has to be '5 or 7 days, or multiples thereof' [8]. There is no agreement on the precise length of treatment but medical textbooks emphasize that therapies should favour treatments of longer duration and that the premature interruption of treatment promotes the evolution of drug resistance [9]. This stems from the idea that overdosing with antibiotics is, at worse, therapeutically neutral and no harm results from taking drugs for prolonged periods. However, mounting clinical [10], experimental [11] and theoretical [12] evidence suggests that short-course therapy can be as effective without imposing selective pressures that favour resistant mutants. These issues have been debated openly in the literature with ensuing disagreement between different communities [13–15]. More recently, the study of Martinez *et al.* [11] is clear in emphasizing treatments 'as brief as clinically appropriate'.

With respect to the optimal dose, current practice indicates that high doses of antibiotics are more effective at suppressing drug-resistant bacteria (discussed in [16]). One argument states that by minimizing population size, we also minimize the probability of occurrence of a *de novo* genetic mutation conferring drug resistance upon bacteria. This is the 'hit early, hit hard' strategy documented as early as 1913, several years before the discovery of penicillin [17].

But high drug concentrations are known to produce side-effects and doses cannot be indiscriminately increased [18]. Not only are high antibiotic dosages toxic [9,19], they can disrupt the ecological stability of the commensal microbiota, allowing pathogens to colonize the host [20]. A strategy for increasing drug potency while decreasing drug concentration is the use of multidrug cocktails [21]. *Synergistic antibiotics*, whereby the combined effect of two drugs is greater than expected given the efficiency of either on their own, have been actively sought for decades [22].

Some have questioned whether aggressive chemotherapies are an appropriate strategy to prevent resistance [23,24]. These studies have shown that if the initial phase of treatment is unsuccessful at clearing the pathogen, then surviving drug-resistant genotypes may thrive in an environment in which many of the drug-susceptible competitors have been eliminated. It has also been shown that synergistic combinations can accelerate the evolution of antibiotic resistance [25] and, as a result, it was suggested that 'antagonistic' drug interactions, seemingly neglected in clinical practice, might slow resistance evolution [26]. In practise, drugs are used even when their synergy is not proved, for example the anti-MRSA combination vancomycin and rifampicin [27,28].

2. A mathematical abstraction

Seeking to understand how mathematics can address questions in antibiotic optimality, we begin with an abstract framework applicable to many mathematical models. From the mathematician's perspective, what we are about to say is self-evident: the optimal control of an adaptive system is unlikely to be realized with control strategies that are constant through time.

To demonstrate more precisely what we mean by this, consider a smooth dynamical law, f, subject to controls, u and v, so that the mathematical model class we analyse has the following form:

$$\frac{\mathrm{d}}{\mathrm{d}t}x = T \cdot f(x, u, v), \quad x(0) = x_0, \quad (2.1)$$

where $x(t) = x(t; u, v) \in \mathbb{R}^n$ is a state variable, $u(t)$, $v(t) \in [0, 1] \subset \mathbb{R}$ are controls and $T > 0$ is a fixed terminal time for antibiotic treatment; u and v represent the dosages of two different antibiotics whose optimal combination we wish to find. Thus, given fixed dosages $u_0 > 0$ and $v_0 > 0$, we let $\theta \in [0, 1]$ denote the relative drug dose, we define an objective functional, J, by

$$J(\theta; T) \stackrel{\text{def}}{=} \int_0^1 (w, x(t; \theta u_0, (1 - \theta)v_0))\mathrm{d}t, \quad (2.2)$$

where $w \in \mathbb{R}^n$ is a weight vector. Here, and throughout, $(\cdot, \cdot)$ denotes Euclidean inner product.

For each u_0, v_0 and $T > 0$, under mild restrictions on f, like smoothness, there is an $\theta_{\mathrm{opt}}(T)$ that satisfies

$$J(\theta_{\mathrm{opt}}(T); T) = \min_{0 \le \theta \le 1} J(\theta; T), \quad (2.3)$$

where the minimum here is taken over a compact subset of the reals: finding the optimal relative drug dose here is a finite-dimensional optimization problem and the existence of a minimizing value of θ is therefore guaranteed.

For u and v to represent antibiotic drugs, we should also assume the following properties:

$$\left(w, \frac{\partial f}{\partial u}(x, u, v)\right) < 0 \quad \text{and} \quad \left(w, \frac{\partial f}{\partial v}(x, u, v)\right) < 0,$$

whenever $u \ge 0$ and $v \ge 0$. In other words, increasing the dose of both drugs will reduce the growth of the microbial population in the components of the weight vector, w.

Definition 2.1 (synergy). Define the 'interaction function'

$$i(\theta) \stackrel{\text{def}}{=} (w, f(x_0, \theta u_0, (1 - \theta)v_0)),$$

and suppose the basal drug concentrations, u_0 and v_0, are calibrated to have equal inhibitory effect: $i(0) = i(1)$. Strict drug synergy is said to hold in (1) when i is convex: $i''(\theta) > 0$ for all $\theta \in (0, 1)$. We define the most synergistic combination, $\theta_{\mathrm{syn}} \in (0, 1)$, to be the value of θ for which the minimum of $i(\theta)$ occurs.

For completeness, we also include the following definition.

Definition 2.2 (antagonism). Suppose that the basal drug concentrations u_0 and v_0 are calibrated to equal inhibitory effect: $i(0) = i(1)$. Strict drug antagonism is said to hold in (1) when the function $i(\theta)$ is concave: $i''(\theta) < 0$ for all $\theta \in (0, 1)$.

Figure 1 illustrates synergy and antagonism that relates these two theoretical definitions to how synergy and antagonism are
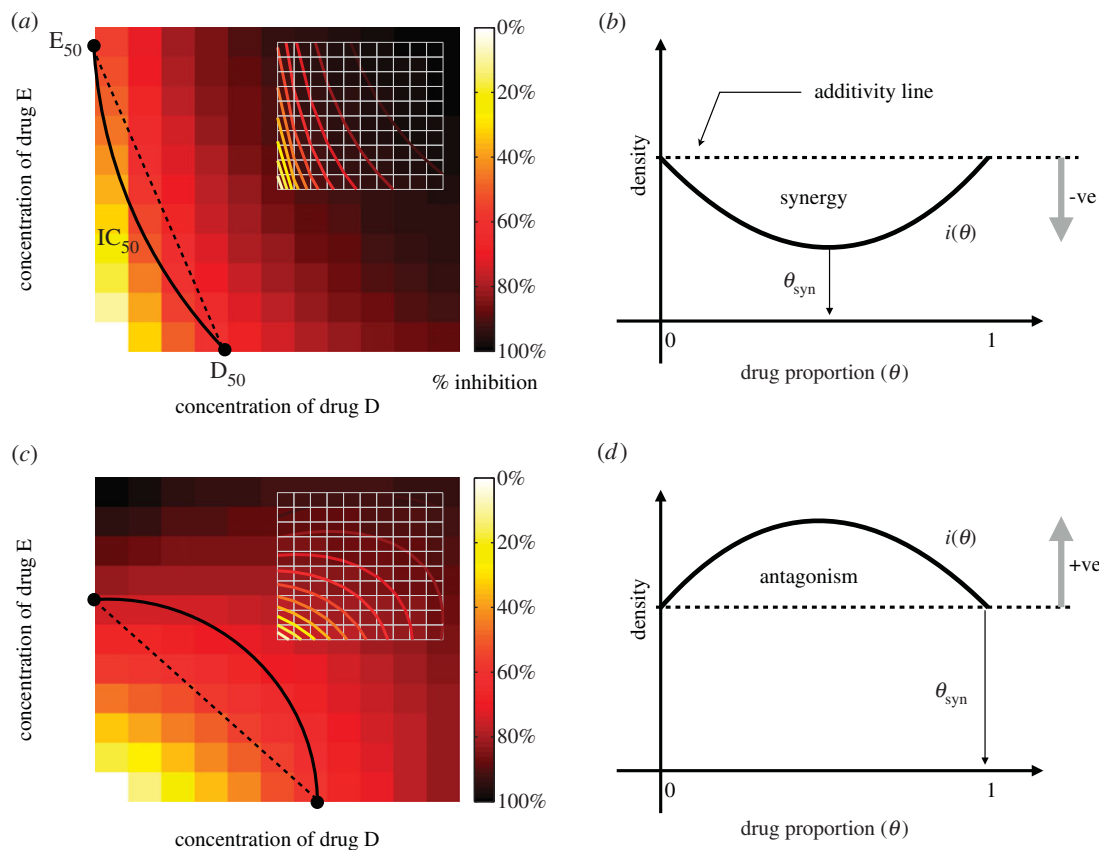
Figure 1. The drug interaction profile, $i(\theta)$, is related to empirical 'checkerboards' that are illustrated in (a,c). In the latter, the concentration of both drugs (called 'D' and 'E') is given on the x- and y-axes, bacterial growth inhibition (or population density or some other fitness measure) is then plotted on the z-axis. The contour of all concentrations that reduce this measure by half is an *isobole* here denoted IC^{50}, and figures (a,c) show two checkerboard plots viewed from above. Basal concentrations of both drugs that achieve the same inhibitory effect in this illustration are D^{50} and E^{50}, θ then parametrizes the equidosage line between these two values. The fitness measure evaluated along this line is shown in (b,d) and we define the degree of interaction based on this curve, this is $i(\theta)$. We say the interaction is *synergistic* when the drug proportion that minimizes $i(\theta)$ satisfies $0 < \theta < 1$ as in (b), we denote the resulting value by θ_{syn}. In (d), we observe $\theta_{\mathrm{syn}=0}$ or $\theta_{\mathrm{syn}=1}$, in this case the drugs are said to be *antagonistic* as $i(\theta)$ is maximized by a drug combination. Adapted from [24]. (Online version in colour.)

seen in empirical datasets known as 'checkerboards'. In practise, the weight w would be chosen so that $i(\theta)$ represents the dependence of total population density on the relative drug proportion, θ.

Suppose that the two drugs in (2.1) are synergistic and proceed by Taylor expanding the functional J with respect to T. If we write solutions of (2.1) as $x = x(t; \theta, T)$, then

$$x(t; \theta, T) = x_0 + tT \cdot f_0(\theta) + \frac{t^2 T^2}{2} L_0(\theta)[f_0(\theta)] + O(T^3),$$

where $f_0(\theta) \stackrel{\mathrm{def}}{=} f(x_0, \theta u_0, (1-\theta)v_0)$ and $L_0(\theta) \stackrel{\mathrm{def}}{=} d_x f(x_0, \theta u_0, (1-\theta)v_0)$ we find

$$\begin{aligned} J(\theta; T) &= \int_0^1 \left(w, x_0 + tT \cdot f_0 + \frac{t^2 T^2}{2} L_0[f_0] + O(T^3) \right) dt \\ &= (w, x_0) + \frac{T}{2}(w, f_0(\theta)) + \frac{T^2}{6}(w, L_0(\theta)[f_0(\theta)]) + O(T^3) \\ &= (w, x_0) + \frac{T}{2} i(\theta) + \frac{T^2}{6} b(\theta) + O(T^3) \\ &= (w, x_0) + \frac{T}{2} \left(i(\theta) + \frac{T}{3} b(\theta) + O(T^2) \right), \end{aligned}$$

(2.4)

where $b(\theta) \stackrel{\mathrm{def}}{=} (w, L_0(\theta)[f_0(\theta)])$. We now define $j(\theta, T) \stackrel{\mathrm{def}}{=} i(\theta) + (T/3)b(\theta) + O(T^2)$ so that $J(\theta, T) = (w, x_0) + (T/2)j(\theta, T)$, the minima of J and j therefore coincide.

From the strict drug synergy property, the minimum of $j(\theta, 0)$ occurs when $\theta = \theta_{\mathrm{syn}} \in (0, 1)$. Moreover, at the minimum of j, there results $(\partial j / \partial \theta)(\theta, T) = 0$, provided T is small enough. As $(\partial^2 j / \partial \theta^2)(\theta_{\mathrm{syn}}, 0) = i''(\theta_{\mathrm{syn}}) > 0$ which is a non-zero quantity by the assumption of strict drug synergy, we may solve $(\partial j / \partial \theta)(\theta, T) = 0$ for θ as a function of T by applying the implicit function theorem. At this solution, $\theta = \theta_{\mathrm{opt}}(T)$, say, and it follows by definition that $\theta_{\mathrm{opt}}(0) = \theta_{\mathrm{syn}}$. Hence, because $(\partial j / \partial \theta)(\theta_{\mathrm{opt}}(T), T) \equiv 0$,

$$i'(\theta_{\mathrm{opt}}(T)) + \frac{T}{3} b'(\theta_{\mathrm{opt}}(T)) + O(T^2) \equiv 0,$$

and, differentiating with respect to T, we establish

$$(\theta_{\mathrm{opt}})'(T)\left(i''(\theta_{\mathrm{opt}}(T)) + \frac{T}{3} b''(\theta_{\mathrm{opt}}(T)) \right) + \frac{b'(\theta_{\mathrm{opt}}(T))}{3 + O(T)} \equiv 0.$$

On setting $T = 0$, it follows that

$$\theta_{\mathrm{opt}}(T) = \theta_{\mathrm{syn}} - \overbrace{\left(\frac{b'(\theta_{\mathrm{syn}})}{3 \cdot i''(\theta_{\mathrm{syn}})} \right)}^{\text{divergence rate:}\,\rho} T + O(T^2),$$

because $(\theta_{\mathrm{opt}})'(0) i''(\theta_{\mathrm{syn}}) + b'(\theta_{\mathrm{syn}})/3 = 0$.

In other words, when we compare with the strategy of optimal drug synergy with the optimal combination, with respect to a wide range of possible measures, provided the genericity condition $(db/d\theta)(\theta_{\mathrm{syn}}) \neq 0$ is satisfied, these two concepts are only close for a period of time that depends

explicitly upon the reciprocal of the strength of synergy of the drug.

2.1. Comments

There are many optimality criteria we could have chosen in (2.3). If we were to let $T > 0$ be free and then define

$$\mathcal{J}(u, v, T) \overset{\text{def}}{=} (w, x(t; u, v, T)),$$

noting that x now depends on T explicitly, one could determine an optimal control (u^*, v^*, T^*) for which

$$\mathcal{J}(u^*, v^*, T^*) = \inf_{u(t) \geq 0, v(t) \geq 0, T \geq 0} \mathcal{J}(u, v, T).$$

This has a larger space of admissible controls than (2.3) and it also includes the terminal time T as an unknown. One could argue that this new functional represents the essential property of what we desire in an optimal antibiotic combination treatment: it determines both the optimal dosages and the terminal time at which to stop treatment.

However, the purpose of continuing to use J as the objective functional here is to yield a set of theoretical predictions that can be tested empirically by reducing the optimal combination question to a one-dimensional problem on the 'equidosage line'. The latter is a line in the two-drug plane of concentrations that is determined by the dosages $(u, v) = (\theta u_0, (1 - \theta)v_0)$, where $0 \leq \theta \leq 1$.

3. An evolutionary experiment

Antibiotic dose–response profiles are usually determined using disc diffusion susceptibility testing [29] or by taking fixed-time (a.k.a endpoint) density measurements in liquid media [30]. Here, we employ the latter because we can use shaken microtitre plate readers to quantify the dynamics of bacterial population densities through time and, based on observed growth kinetics, thereafter determine drug susceptibility at different antibiotic dosages.

In the following, we use a standard batch-transfer experimental protocol (see appendix A) to treat bacteria. This is often used to study adaptation to antibiotic environments [24,25], whereby a shaken environment with liquid growth medium is inoculated with bacteria that are cultured in an array of wells for a fixed period of time. Population densities are measured continually for 24 h at which time a fixed volume is sampled from the flask and transferred to a new well containing fresh growth medium and antibiotics. The repetition of this process defines the batch-transfer protocol.

In the remainder, we have two antibiotics at concentrations denoted by $D(t)$ and $E(t)$ at time t. We use $B(t) = (B^{(1)}(t), \ldots, B^{(n)}(t))$ for the vector containing the density of n bacterial phenotypes differing in their dose–response profiles and $S(t)$ will denote the concentration of an essential but limiting carbon source supplied to the bacteria.

Each experiment consists of N transfers. If each transfer has a duration of T hours, with $t \in [0, T]$, the state of the system at any time is

$$x_i(t) \overset{\text{def}}{=} (B_i(t), S_i(t), D_i(t), E_i(t)),$$

where a subscript has been placed on B to denote the phenotypic densities each day and so $i = \{1, 2, \ldots, N + 1\}$. The initial density of bacteria after transfer i is a small proportion of the terminal state of the previous day and, as illustrated in
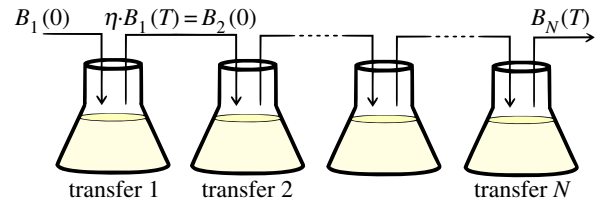

Figure 2. Schematic illustration of a batch-transfer experiment. A small population of bacteria is inoculated and cultured under essential resource limitation for N units of time. Then, a fraction η of the population is transferred to a new flask containing fresh medium and antibiotics and the process is repeated for several days. (Online version in colour.)

figure 2, if $0 < \eta \ll 1$ denotes this proportion then the initial condition of transfer $i > 1$ will satisfy

$$B_i(0) = \eta \cdot B_{i-1}(T),$$

where $B_1(0) = (B_0, 0, \ldots, 0)$ is the density vector of the bacteria on the first day. In practise, B_0 will represent around 10^5 cells per millilitre in any one of our experimental protocols that are described later.

The population dynamics of the bacteria competing in this environment can be written as a single differential equation

$$\frac{\mathrm{d}}{\mathrm{d}t} x_i = F(x_i, D_i, E_i), \tag{3.1a}$$

where F is a model-specific mapping described in §3.3 and the initial condition

$$\begin{aligned} x_i(0) &= (B_i(0), S_i(0), D_i(0), E_i(0)) \\ &= (\eta \cdot B_{i-1}(T), S_0, D_0, E_0) \end{aligned} \tag{3.1b}$$

applies each day where $x_1(0) = (B_1(0), S_0, D_0, E_0)$. Here, S_0 is a fixed parameter denoting the initial concentration of the limiting resource each day, D_0 and E_0 are also fixed and represent the basal concentrations of antibiotic supplied.

3.1. Modelling the action of bacteriostatic antibiotics

The bacteriostatic antibiotics we use suppress the bacterial growth rate by inhibiting protein synthesis and we represent the action of the drug by viewing it as a suppressor of biomass synthesis. So, suppose each cell ingests the essential resource from the environment as a process following Monod kinetics:

$$u(S) = \frac{V_{\max} S}{K + S}, \tag{3.2}$$

where $V_{\max}$ represents the maximal resource uptake rate and K is a half-saturation constant.

The growth rate of each bacterium depends on the concentration of antibiotic present in the environment, so we assume the above uptake function is modulated by an antibiotic-dependent coefficient $c(D)$ that converts units of the limiting resource to biomass and describes the efficiency of cell production per unit resource in the presence of antibiotic. Thus, the per-cell, per-unit time growth rate can be written as $G(S, D) = u(S) \cdot c(D)$. We will write $c(D)$ as a product of the cell conversion rate in a drug-free environment, c, and a dimensionless inhibition coefficient that depends on the concentration of antibiotics

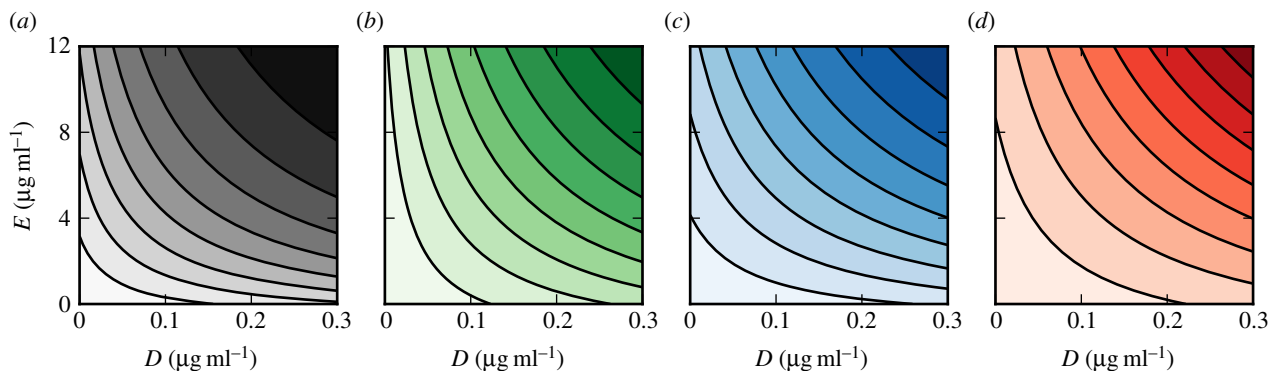$$G(S, D) = c\, u(S) \gamma(D). \tag{3.3}$$

Figure 3. Contour plots of the drug inhibition surface $\gamma(D, E)$ for different bacterial phenotypes (parameter values contained in table 1). Each line represents a 10% decrease of growth rate at a fixed concentration of resource ($S_0 = 2000\ \mu g\ ml^{-1}$). (*a*) Susceptible phenotype, (*b*) E-resistant, (*c*) D-resistant and (*d*) multidrug, DE-resistant bacteria. (Online version in colour.)

Forms for $\gamma(D)$ can be derived using standard enzymatics [31] and if we suppose that the antibiotic suppresses growth due to a competitive inhibition process, then the following expression is consistent [31] with antibiotic-target binding data for rifampicin-like drugs:

$$\gamma(D) \stackrel{\text{def}}{=} 1 - \frac{\kappa_1 D}{1 + \kappa_2 D}, \qquad (3.4)$$

where κ_1 and κ_2 are parameters characterizing susceptibility to the antibiotic.

3.2. Multidrug interactions in a model cell

To extend the rationale of §3.1, assume two antibiotics are present in the environment at concentrations D and E. Again, bacterial growth is modelled as a Monod term multiplied by a growth inhibition coefficient, $\gamma(D, E)$, so $G(S, D, E) = c\ u(S)\gamma(D, E)$, where c is a conversion rate and $u(S)$ is the resource uptake function defined in equation (3.2).

Now, $\gamma(D, E)$ is a function, whereby $\gamma(D, 0) = \gamma_D(D)$ and $\gamma(0, E) = \gamma_E(E)$, and $\gamma_D(D)$ and $\gamma_E(E)$ are inhibition functions describing the action of each antibiotic deployed alone.

The shape of the contours of $\gamma(D, E)$ determines the antibiotic interaction [32]. In particular, we use two bacteriostatic antibiotics of different functional classes with a known synergistic interaction [24,25]: *erythromycin* (E), a macrolide that binds to the 50S ribosomal RNA subunit and *doxycycline* (D), a tetracycline that binds to the 30S ribosomal RNA subunit. As these drugs have non-overlapping targets, we model their interaction as non-exclusive competitive inhibitors [33] and the growth inhibition coefficient for a multidrug combination of D and E is

$$\gamma(D, E) \stackrel{\text{def}}{=} \frac{1}{1 + \kappa_d D + \kappa_e E + \kappa_m D E}, \qquad (3.5)$$

where κ_d, κ_e and κ_m are positive constants. Note that κ_m controls the strength of synergy and if it is zero, the drug interaction is additive.

Assuming cell yield (defined as the maximal cells produced per essential resource) is the same for four genotypes (drug-susceptible wild-type, D-resistant, E-resistant and DE-resistant), the growth rate and antibiotic susceptibility patterns for different bacterial strains will be characterized in terms of a vector of parameters, $(V^*_{max}, K^*, \kappa^*_e, \kappa^*_d, \kappa^*_m)$, where the asterisk is a placeholder for the genotype under consideration. For instance, we will denote an *antibiotic-susceptible*

bacterial wild-type with the superscript s and its growth rate will be written as

$$G^s(S, D, E) = c \left(\frac{V^s_{max} S}{K^s + S} \right) \left(\frac{1}{1 + \kappa^s_d D + \kappa^s_e E + \kappa^s_m D E} \right).$$

By contrast, a *multidrug-resistant* mutant (represented by a superscript m) would have, by definition, a higher growth rate than susceptible bacteria at high concentrations of antibiotics. Thus, if the growth rate of a multidrug-resistant mutant is given by the function

$$G^m(S, D, E) = c \left(\frac{V^m_{max} S}{K^m + S} \right) \left(\frac{1}{1 + \kappa^m_d D + \kappa^m_e E + \kappa^m_m D E} \right),$$

then, to represent greater resistance, there must exist a critical drug combination (D^*, E^*) for which

$$G^m(S, D, E) > G^s(S, D, E) \quad \text{for all } D \geq D^* \text{ and } E \geq E^*.$$

Antibiotic resistant cells often encounter a reduction in fitness in an antibiotic-free environment, a so-called *fitness cost of resistance* [34]. In our framework, this can be realized by imposing a lower resource uptake rate and, therefore, a lower growth rate in an antibiotic-free environment

$$G^m(S, 0, 0) < G^s(S, 0, 0).$$

As an illustration, figure 3 contains the contour plots of growth functions, $G^*(S, D, E)$, at fixed resource concentrations but at different drug doses for susceptible, single-drug-resistant and multidrug-resistant bacterial genotypes; there are four such functions G^s, G^d, G^e and G^m, one for each genotype. Note how the contour lines are concave in all four cases and, therefore, the drug interaction is synergistic for each genotype.

3.3. Resistance mutations

Susceptible bacteria can acquire resistance through the horizontal transfer of mobile genetic elements [35], through single point mutations in drug targets [36] or through the amplification of genomic regions containing resistance genes [37]. Seeking to understand how target modification affects the optimality properties of antibiotic combinations, we model resistance adaptation by allelic changes in two independent genetic loci.

Susceptible genotypes evolve resistance due to point mutations occurring at rate $\epsilon > 0$ (per cell per division) in an 'E-resistance' locus and a 'D-resistance' locus. The accumulation of two mutations confers multidrug resistance. The
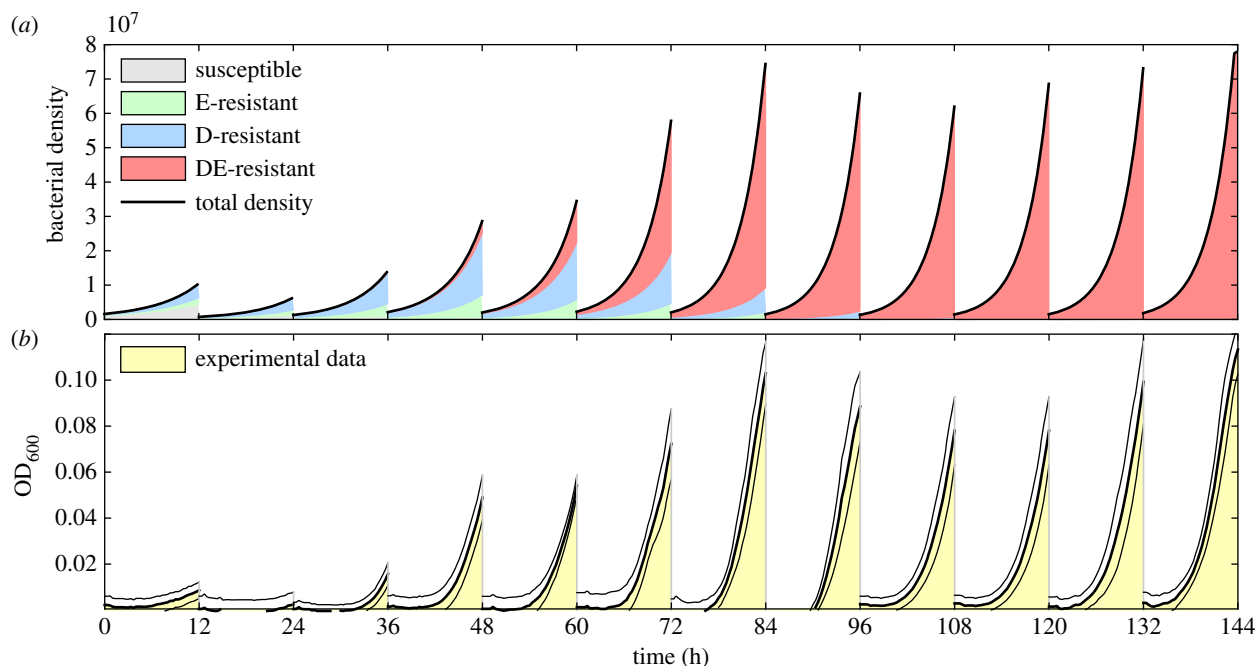
Figure 4. Adaptation to multidrug environments in a batch transfer experiment. *Escherichia coli* is cultured for 12 h before propagating a fraction of the terminal population into the next season (*a.k.a* transfer) containing fresh growth medium and both antibiotics. (top) A simulation of the model defined by (3.1) and (3.6) using parameter values in table 1. The four different shaded areas represent densities of each of the bacterial genotypes (where there is one for drug-susceptible, then E-resistant, D-resistant and multidrug-resistant mutants). (bottom) Optical densities obtained experimentally (*E. coli* AG100 cultured in 7 μg ml^{-1} erythromycin and 0.3 μg ml^{-1} of doxycycline), the areas shown show the mean growth dynamics of eight replicates whereas the lines denote standard errors at each time point. (Online version in colour.)

mutation structure on these loci can be described by a mutational matrix

$$\mathcal{M}_\epsilon \stackrel{\text{def}}{=} (1 - \epsilon)I + \epsilon M.$$

Here, I is the identity matrix, ϵ the rate of mutation and M is a stochastic matrix whose entries, m_{ij}, control the rate at which bacterial type j mutates into bacterial type i.

If 1 denotes a vector of ones of the appropriate dimension, then the mutational matrix is stochastic

$$1^T \mathcal{M}_\epsilon = 1 \quad \text{and} \quad 1^T M = 1.$$

We assume M (and therefore $\mathcal{M}_\epsilon$) is *irreducible* in the sense that for each pair (i,j), there is a number $p = p(i, j)$ such that the (i,j)th entry of M^p is non-zero.

Our model will be completed when we describe the mapping, F, in (3.1a) that defines the ecological setting for the above genetics. We are modelling the densities of four different genotypes: a susceptible wild-type at density B_i^s, B_i^d and B_i^e are resistant mutants to drugs D and E, respectively, and B_i^m is the multidrug-resistant mutant. We then define a vector that contains the densities of each strain,

$$\boldsymbol{B}_i(t) \stackrel{\text{def}}{=} (B_i^s(t), B_i^e(t), B_i^d(t), B_i^m(t)),$$

and the dynamics (at transfer i) of this two-allele, two-locus model can be written as

$$\frac{\mathrm{d}}{\mathrm{d}t} \boldsymbol{B}_i = \mathcal{M}_\epsilon(G(S, D, E) \cdot \boldsymbol{B}_i), \quad (3.6a)$$

$$\frac{\mathrm{d}}{\mathrm{d}t} S = -(u(S), \boldsymbol{B}_i), \quad (3.6b)$$

$$\frac{\mathrm{d}}{\mathrm{d}t} D = -\mathrm{d}D \cdot (B_i^s + B_i^d + B_i^e + B_i^m) \quad (3.6c)$$

and

$$\frac{\mathrm{d}}{\mathrm{d}t} E = -eE \cdot (B_i^s + B_i^d + B_i^e + B_i^m). \quad (3.6d)$$

Here, $G(S, D, E)$ is the vector (G^s, G^d, G^e, G^m) and the dot in (3.6a) denote pointwise multiplication. The parameters d and e are binding constants of each antibiotic to each bacterial genotype and the parentheses in (3.6b) denote the standard Euclidean inner product.

Figure 4 illustrates a simulation of equation (3.1), as defined by equation (3.6), where the transfer occurs every 12 h and an ED-combination treatment has been used. As the number of transfers increases, the multidrug-resistant ED-genotype (shown in red) outcompetes the other genotypes and we see expected behaviour in that this genotype sweeps through the population as it adapts to the presence of both drugs. For comparison, figure 4b shows experimental data obtained for *Escherichia coli* adapting to a multidrug environment that contains 7 μg ml^{-1} erythromycin and 0.3 μg ml^{-1} of doxycycline where total population density is shown for each transfer.

4. Preliminary results

4.1. Population heterogeneities and non-monotonic dose–response

Antimicrobial susceptibility tests can be difficult to standardize [38], but they are widely used to determine important quantitative pharmacodynamic parameters characterizing the inhibitory relationship between antibiotic and bacteria [39]. For bacteriostatic antibiotics, a dose–response curve that showing densities at a given timepoint at a series of increasing dosages characterizes the effect of the drug. An important feature of this is the so-called minimum inhibitory concentration. This is the lowest drug dosage at which a 99.9% reduction in
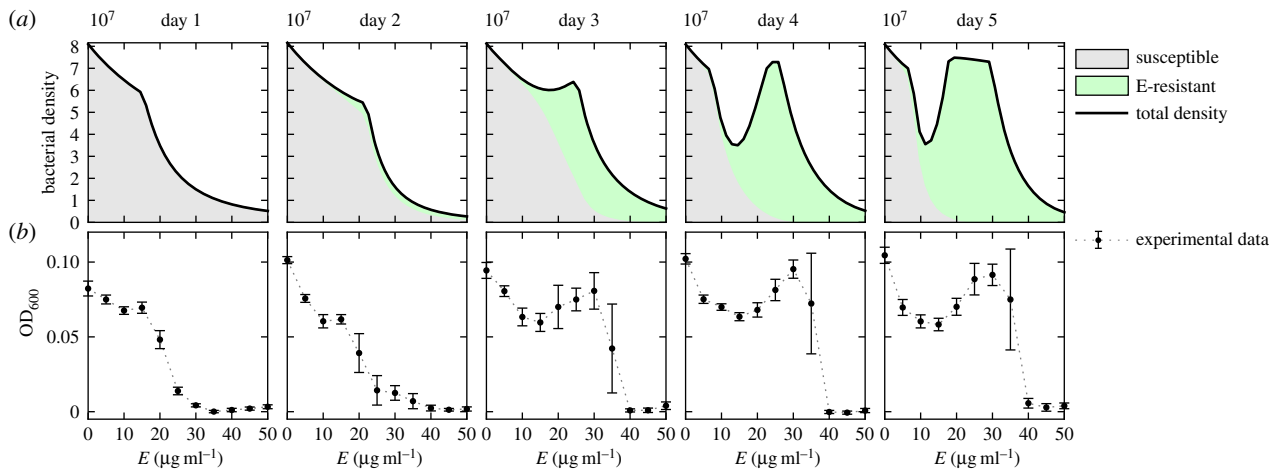
Figure 5. Non-monotonic dose–response curves in serial-transfer experiments. Row (*a*) illustrates simulations of a model based on (3.6) (using parameters in table 1), whereas row (*b*) illustrates optical densities of *E. coli* (strain AG100) measured at 24 h intervals at different concentrations of the drug erythromycin (E). Each column shows a dose–response curve for each day. Note how the characteristic, monotone dose–response curve of day one becomes a non-monotone curve due to a sub-population of resistant phenotypes that emerge more quickly at higher doses (error bars here and throughout denote standard error, eight replicates). (Online version in colour.)

bacterial density can be achieved at that timepoint by the use of the drug. By the very nature of antibiotics, we expect dose–response data to be monotonic decreasing.

We therefore evaluated the effect of resistance adaptation on the dose–response curve with the following experiment. A clonal population of *E. coli* bacteria (several different strains were used) was inoculated into a 96-well microtitre plate containing different concentrations of a single bacteriostatic antibiotic, in this case erythromycin, at a concentration E measured in $\mu g\ ml^{-1}$. After 24 h, following the batch-transfer protocol, we transferred a small volume from each well into an identical plate but with fresh growth medium and antibiotics. We repeated this procedure for 5 days (see appendix A for more detailed experimental methods).

Figure 5*b* illustrates the population densities at the end of each day in this protocol (density here is the optical density of the population measured at a 600 nm wavelength).

The first day's dose–response curve has the common characteristic to these datasets: first a plateau, then a sharp drop as the dose increases. By the second day, there appears to be a small protuberance at intermediate drug concentrations. As the experiment proceeds, this protuberance is more pronounced, eventually producing a non-monotonic dose–response curve. This phenomenon is related to the Eagle effect that was first described in 1948 where non-monotonic dose–response relationships were noted at low cell densities [40].

Equations (3.6*a*–*d*) provide a mechanistic explanation of the observed non-monotonicity in the dose–response curve. Simulations of the model (implemented without doxycycline, so that $D(t) \equiv 0$) shown in figure 5*a* illustrate how intermediate drug concentrations support coexistence between the susceptible strain (the grey area) and the E-resistant strain (the green area; E for erythromycin). By contrast, the fitness cost paid by the resistant cells at low antibiotic concentrations is large enough that this environment selects the susceptible bacteria, while at high drug doses only the resistant phenotype is able to persist. While this is not the same observation as that made by originally by Eagle in 1948, it might be appropriate to call this phenomenon an 'adaptive Eagle effect' as it only appears after the initial population has adapted to the presence of the drug.

It is noteworthy that this unusual behaviour of an adaptive dose–response profile can be captured by such simple genetical and ecological assumptions, this gives us some confidence that the model is able to capture features that might not be evident from verbal reasoning alone.

4.2. Multidrug interactions are dynamic

The standard test used to determine the degree of interaction of a pair of antibiotics is a two-dimensional dose–response surface known as a checkerboard [41]. The horizontal axes are the dosages of the drugs and the vertical, *z*-axis represents the density of the bacterial population measured experimentally at some time. Based on the shape of the lines of equal inhibitory effect in the checkerboard that are known as isoboles, one characterizes the interaction between the two drugs as follows [22]: if the isoboles are convex the interaction is synergistic, if they are concave the drugs are antagonistic.

We performed a checkerboard experiment (using 256 different drug combinations with 11 replicates, see appendix A) using erythromycin (E) and doxycycline (D), drugs with an established synergy [25]. As expected, the isoboles exhibited the characteristic of a synergistic interaction as can be seen in the bottom-left panel of figure 6*a*. We then took samples of bacteria from this experiment containing a highly synergistic combination ($E_0 = 4.8\ \mu g\ ml^{-1}$, $D_0 = 0.08\ \mu g\ ml^{-1}$) and used these to inoculate a new batch-transfer experiment. After four daily transfers, we used the resulting evolved bacterial populations to determine another checkerboard, the purpose of which was to determine how the adaptation to a synergistic environment would be manifested within the isoboles of the dose–response surface.

Figure 6 shows that the checkerboard has shifted in the sense that higher densities are produced at higher drug concentrations, consistent with drug-resistance adaptation. However, the data in figure 6 are too coarse to allow a conclusive analysis on whether the synergy that was present on day 1 still remains 4 days later. It is probably unwise to scrutinize the subtleties of this surface too closely in terms of how it relates to the nature of the drug interactions, the data being as sparse as it is. In order to address our question,
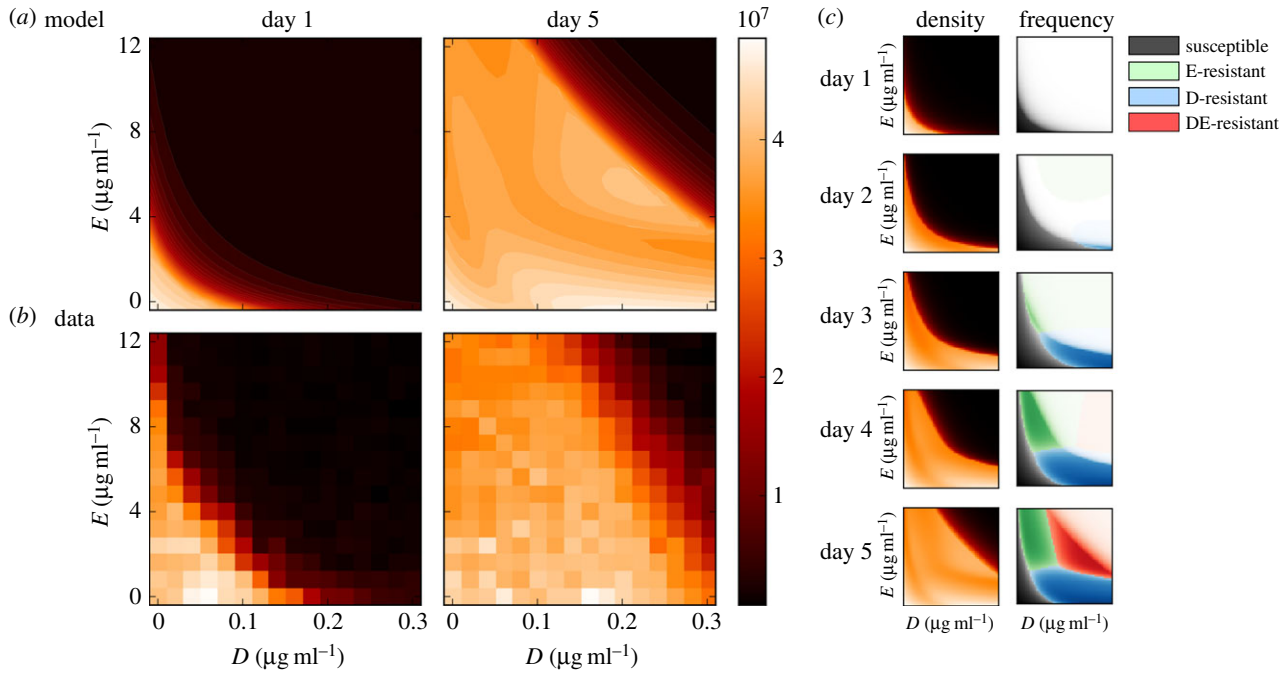
Figure 6. Empirical and theoretical checkerboards. (*a*) A dose–response surface, or isobologram, of *E. coli* MG4100 grown in a glucose-limited environment under the effect of different concentrations of doxycyline (D) and erythromycin (E) when measured on days 1 and 5 (11 replicates). (*b*) Numerical simulations of the two-locus, two-allele model (parameters in table 2) illustrates the dynamic nature of the population structure. Boxes (*c*) show bacterial genotypes with the highest frequency with colour intensity proportional to the density of each type. By day 5, the multidrug-resistant genotype ('DE-resistant') has the highest density at high drug concentrations, at low concentrations the susceptible has the highest densities and the single-drug-resistant phenotypes (E-resistant and D-resistant) are over-represented near each axis. (Data first appeared in [24], the analysis and interpretation is new.) (Online version in colour.)
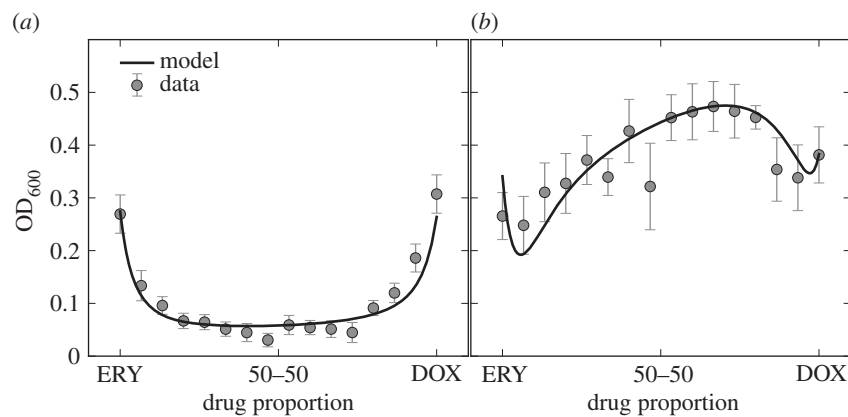

Figure 7. The smile–frown transition in optical density data. Both figures show optical density of *E. coli* MG4100 as a function of the variable θ, the relative drug concentration: $\theta = 1$ corresponds to DOX and $\theta = 0$ corresponds to ERY. The left-hand figures shows, after 12 h (*a*) growth, that these two drug act synergistically on the population, whereas the 36 h (*b*) data shows an antagonistic profile. At 12 h, population density is minimized by a drug combination because of the synergy, whereas at 36 h the same combination maximizes population densities. (This dataset appeared in [24], the model fit to that data is new.)

we use a different analysis technique that gives more precise information on the drugs' interaction.

4.3. A two-locus, two-allele smile–frown transition

Our definition of synergy and antagonism is stated in terms of two possible instances of the function $i(\theta)$ in definitions 2.1 and 2.2. In these definitions, a convex form for $i(\theta)$ corresponds to synergy, a concave $i(\theta)$ corresponds to antagonism. However, a phenomenon can arise, whereby synergism is lost and in [24] this was termed the 'smile–frown transition'.

In this transition, a short-term synergy is replaced by an antagonism in the data because the most potent combinations select most for drug-resistant genotypes. As a result, the

population density data are 'inverted' and the characteristic, convex U-shape of synergy gives way to a near-concave W-shaped pattern that represents an antagonism. The population density data in figure 7*a,b*, respectively, show this transition both in data and in an instance of the population genetics model presented above.

The relevance of this observation, made of population-level data, can be understood in the context of the 'search for synergy' [22] if we re-visit the growth functions, $G^*(S, D, E)$, used in equation (3.6). According to that model, the function $\theta \mapsto G(S, \theta D, (1 - \theta)E)$ is convex (i.e. synergistic) for all S, D and E (figure 3) and yet the population-level outcome that results from simulating this model need not respect that synergy because of a population structure that arises during treatment (figures 6 and 7). One could interpret this

by stating that single-cell synergy does not imply an 'evolutionarily robust population synergy'.

Informally, the changing drug interaction pattern in figure 7 could be seen as two conjoined copies of the data from figure 5 in the sense that the smile–frown transition is due to two emerging, non-monotone dose–response profiles laid contiguously, side by side.

4.4. The optimal drug combinations can depend upon treatment duration

The subtle, frequency- and density-dependent effects that produce non-monotone dose–responses and the smile–frown transition suggest that what dose and combinations are optimal for a treatment that lasts 1 day might be different from a treatment that lasts longer.

To address this, we need to define what we mean by an optimal treatment: an *optimal drug combination* needs an objective. In our context, we could use a criterion that measures the inhibitory effect of an antibiotic using, perhaps, only on the total density of bacteria found at the end of the experiment. Or else, we could measure the totality of bacterial cells produced by each treatment. These measures, however, only account for bacterial yield and could therefore completely fail to capture the reduction of growth rate induced by a bacteriostatic antibiotic.

Indeed, two experiments can have similar final bacterial densities but with very different growth dynamics to achieve those densities.

To overcome this, we use an optimality measure of treatment success that incorporates the total observed bacterial density in an experiment of N days in an objective functional and we will refer to this as the *cumulative area under the curve* (AUC), $\mathcal{A}$, defined as follows:

$$\mathcal{A}(N; D, E) \stackrel{\text{def}}{=} \sum_{i=1}^{N} \int_0^{24\text{h}} B_i(t; D, E)\mathrm{d}t. \qquad (4.1)$$

Experimentally, this quantity can be approximated by measuring bacterial density continually and then applying a numerical integration rule over the empirically determined daily growth curves. In our experiments, this is done every 20 min thus producing a timeseries of population densities each day, labelled i, that depends on the drugs used, (D, E). The population density timeseries is therefore written as $B_i(t; D, E)$.

We normalize this measure with respect to a drug-free control population and so compute *AUC inhibition*, a dimensionless performance index we refer to in the remainder as $\mathcal{I}$

$$\mathcal{I}(N; D, E) \stackrel{\text{def}}{=} 1 - \frac{\mathcal{A}(N; D, E)}{\mathcal{A}(N; 0, 0)}. \qquad (4.2)$$

This objective functional takes values in the interval $[0,1]$ and if $\mathcal{I}(N; D, E) = 1$, the antibiotics have completely inhibited bacterial growth, if $\mathcal{I}(N; D, E) = 0$ the drugs have no effect.

To make a comparison between the efficacy of different drug cocktails a fair one, we perform the following calibration. We determine 'basal' concentrations of erythromycin and doxycycline from their single-drug dose–response curves so that each drugs' monotherapy achieves equal inhibitory effect on growth at 24 h. So, if we denote by E_0 and D_0, those basal concentrations, respectively, we then represent fixed-dose

combinations of the two drugs by a dimensionless drug proportion coefficient, θ. Each drug combination used to treat bacteria experimentally therefore lies on the equidosage line $(\theta D_0, (1 - \theta)E_0)$, where $0 \leq \theta \leq 1$.

The drug proportion θ remains constant throughout the experiment and, therefore, any bacterial population is initially exposed to the same, fixed-dose multidrug concentrations throughout the treatment. This assumption, however, does not imply that the environmental drug concentration remains constant at all times because concentrations decrease as drug molecules enter the cell and bind to their targets. Antibiotic molecules also degrade naturally over time in solution.

We now take θ to be our control variable and define the *optimal drug proportion* to be the combination that maximizes the objective functional $\mathcal{I}$ in (4.2), a quantity we denote θ^*. The optimal drug proportion is now determined by solving the following one-dimensional optimization problem:

$$\mathcal{I}(N; \theta^* D_0, (1 - \theta^*)E_0) = \max_{\theta \in [0,1]} \mathcal{I}(N; \theta D_0, (1 - \theta)E_0). \qquad (4.3)$$

Now, by definition of synergy, the short-term, $N = 1$, optimal drug combination for this synergistic drug pair must correspond to the combination that maximizes the synergistic effect. Thus, a near 50–50 combination treatment should be optimal when $N = 1$, this would be represented by the optimal control residing at, or close to $\theta^* = 1/2$.

However, does this synergistic value for the optimum remain so for a longer term experiment, when $N > 1$? We expect that for each $N \geq 1$, there is an associated optimal value, $\theta^*(N)$ and by virtue of the synergy $\theta^*(1) \approx 1/2$. We now address the behaviour of this function as measured experimentally using a batch-transfer protocol as N grows.

Figure 8 is a representation of an empirical and a theoretical dataset, giving a comparison of the optimal combination obtained experimentally (figure 8*b*) with the optimal combination computed using the two-locus, two-allele model defined by equations (3.6*a*–*d*) (figure 8*a*). As expected from the synergy, in both cases the optimal 1-day drug proportion corresponds to the drug combination that maximizes synergy, but the optimal drug proportion changes when we treat for longer durations. For example, if we wanted a treatment lasting 5 days, it is then preferable according to our measure of success to deploy a single drug instead of a two-drug cocktail.

5. Conclusion

We have shown that an optimal drug combination can depend on the duration of the treatment (the parameter N above). So, for each treatment of length N, there is control strategy (a.k.a. relative drug combination) $\theta^*(N)$ that is optimal, moreover $\theta^*(N)$ is not a constant function of N. This result is not surprising from a theoretical control perspective as complex, adaptive systems are unlikely to be controlled optimally using constant, non-responsive controls. Note that we have not determined the optimal treatment, we have only demonstrated that the optimal combination along the equidosage line depends on the length of treatment.

Although this is a laboratory study data analysed using a model inspired by drug target modification, there are other ways in which bacteria resist antibiotics. Resistance to erythromycin and doxycycline is also conferred by the product of an operon *acrRAB* and the gene *tolC* that form an efflux pump
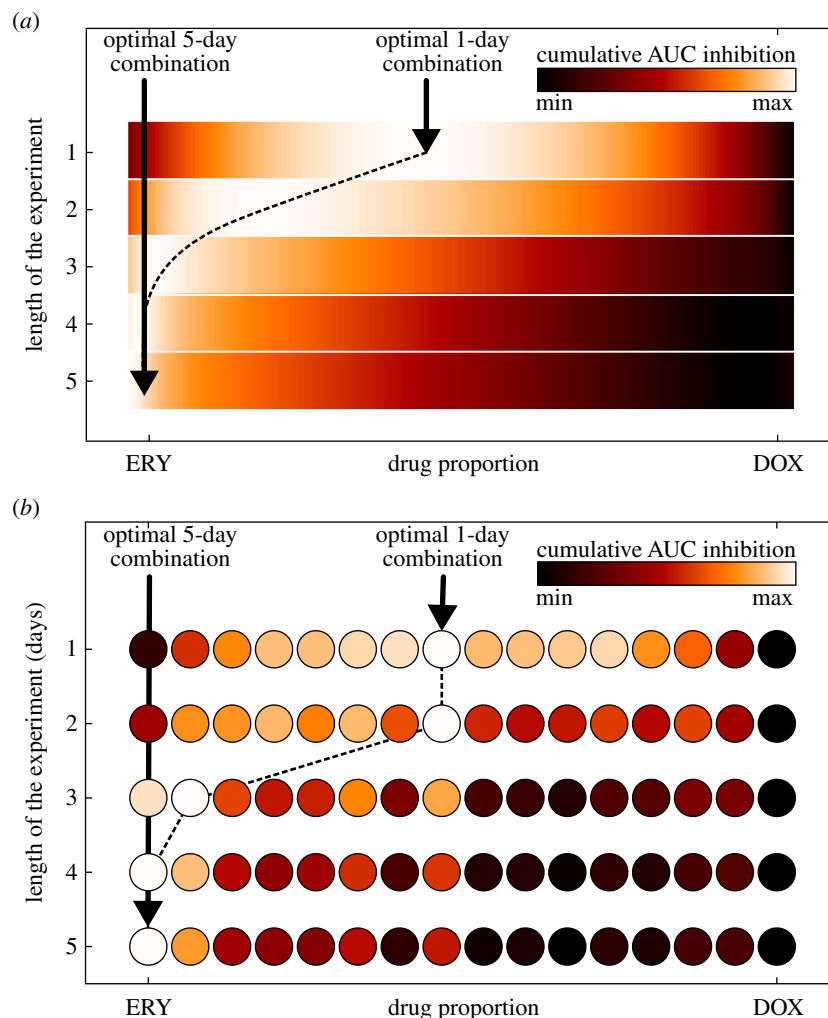
Figure 8. The optimal drug combination depends on the length of the experiment. The optimal drug combination as a function of the length of the experiment: the colour gradient represents the normalized cumulative AUC inhibition (white represents maximum inhibition, and black the minimum inhibition) of *E. coli* MG4100. The dotted line corresponds to the optimal drug proportions as a function of the length of the experiment. (*a*) Simulations of the theoretical, two-locus, two-allele model from (3.6) using parameters in table 2. (*b*) Empirical data: each circle represents a different drug proportion tested experimentally. Note how, both in the experiment and the model, at the beginning of the experiment the optimal treatment corresponds to the combination treatment that maximizes synergy, but for longer treatments the model and the data coincide in the sense that the optimal strategy uses more and more erythromycin. In an experiment of 5 days, it would have been better not to combine the drugs at all, at least according to this optimality measure. (Online version in colour.)

spanning the inner membrane, periplasm and outer-membrane in *E. coli*. Treating with these drugs is known to lead to genomic duplication events where around 8% of the *E. coli* genome is duplicated in which *acrRAB* is sited [24]. A contribution of this study is to show that the smile–frown transition of the previous study [24] can be realized theoretically by target modification, not only by pump duplications.

Nevertheless, although we have not tested the idea directly, our data indicate that actively changing the antibiotics used during treatment, or changing the way they are combined, may be one path to explore further at higher dosages. *Mycobacterium tuberculosis* is, in some sense, treated in this way [42] but it might also be possible that other pathogens could be treated successfully with regimens that change through time, but such sequential regimens are not common. There is clinical evidence to show that sequential treatments of *Helicobacter pylori* can outperform combination treatments at the same dose [43,44], although not all trials have been equally successful [45].

Clinicians are well in advance of our theory, having trialled a range of strategies to combat resistance evolution. The recent development of personalized, rapid-diagnosis

devices to determine the pathogen responsible for infection with patient-specific, DNA-based testing so the most appropriate drug can be given as soon as possible [46,47] is one such advance. For a review of the many protocols trialled in practice, see [48]. However, there could be a role for data-driven optimal control theory that can highlight new strategies in the search for treatments that help combat resistance.

Appendix A. Experimental methods

Escherichia coli K12 (strains AG100 and MC4100) were used throughout and cell inoculations were taken from the same colony of each strain for all the experiments conducted. Experimental populations were cultured in M9 medium at 30°C with the following concentrations: part A: 350 g l^{-1} K_2HPO_4, 100 g l^{-1} KH_2HPO_4; part B: 29.4 g l^{-1} trisodium citrate, 50 g l^{-1}(NH_4)$_2SO_4$, 5 g l^{-1}MgSO4. Parts A and B

Table 1. Parameter values for *E. coli* strain AG100.

parameter	description	value
S_0	glucose supply	2000 µg ml^{-1}
D_0	basal concentration of drug D	0.3 µg ml^{-1}
E_0	basal concentration of drug E	7 µg ml^{-1}
V_{max}^i	maximal carbon uptake rate	$V_{max}^s = 8.6 \times 10^{-6}$, $V_{max}^e = 8.5 \times 10^{-6}$
	of bacterial type i (µg cell^{-1} h^{-1})	$V_{max}^d = 8.58 \times 10^{-6}$, $V_{max}^m = 8.5915 \times 10^{-6}$
K	bacterial half-saturation constant	0.0527 µg ml^{-1}
c	resource conversion	2.18×10^4 cell µg^{-1}
d	drug D binding rate	1.469×10^{-9} µg cell^{-1}
e	drug E binding rate	1.44×10^{-9} µg cell^{-1}
κ_*^s	inhibition of B^s (ml µg^{-1}, ml µg^{-1}, (ml µg^{-1})^2, resp.)	$\kappa_e^s = 0.03002$, $\kappa_d^s = 0.6097$, $\kappa_m^s = 0.8080$
κ_*^e	inhibition of B^e (ml µg^{-1}, ml µg^{-1}, (ml µg^{-1})^2, resp.)	$\kappa_e^e = 0.004351$, $\kappa_d^e = 0.5097$, $\kappa_m^e = 0.2512$
κ_*^d	inhibition of B^d (ml µg^{-1}, ml µg^{-1}, (ml µg^{-1})^2, resp.)	$\kappa_e^d = 0.015097$, $\kappa_d^d = 0.2418$, $\kappa_m^d = 0.23596$
κ_*^m	inhibition of B^m (ml µg^{-1}, ml µg^{-1}, (ml µg^{-1})^2, resp.)	$\kappa_e^m = 0.0015097$, $\kappa_d^m = 0.0590$, $\kappa_m^m = 0.02581$
ϵ	rate of point mutations	10^{-4} per locus per cell per division
η	dilution parameter	1% of biomass

Table 2. Parameter values for *E. coli* strain MC4100.

parameter	description	value
S_0	glucose supply	2000 µg ml^{-1}
D_0	basal concentration of drug D	0.15 µg ml^{-1}
E_0	basal concentration of drug E	9 µg ml^{-1}
V_{max}^i	maximal carbon uptake rate	$V_{max}^s = 2.778 \times 10^{-6}$, $V_{max}^e = 2.289 \times 10^{-6}$
	of bacterial type i (µg cell^{-1} h^{-1})	$V_{max}^d = 2.2839 \times 10^{-6}$, $V_{max}^m = 2.389 \times 10^{-6}$
K	bacterial half-saturation constant	0.0527 µg ml^{-1}
c	resource to biomass conversion	2.851×10^4 cell µg^{-1}
d	drug D binding rate	1.469×10^{-9} µg cell^{-1}
e	drug E binding rate	1.44×10^{-9} µg cell^{-1}
κ_*^s	inhibition of B^s (ml µg^{-1}, ml µg^{-1}, (ml µg^{-1})^2, resp.)	$\kappa_e^s = 0.03453$, $\kappa_d^s = 2.3802$, $\kappa_m^s = 3.0928$
κ_*^e	inhibition of B^e (ml µg^{-1}, ml µg^{-1}, (ml µg^{-1})^2, resp.)	$\kappa_e^e = 0.02134$, $\kappa_d^e = 1.8802$, $\kappa_m^e = 0.0241$
κ_*^d	inhibition of B^d (ml µg^{-1}, ml µg^{-1}, (ml µg^{-1})^2, resp.)	$\kappa_e^d = 0.02484$, $\kappa_d^d = 0.19512$, $\kappa_m^d = 0.331$
κ_*^m	inhibition of B^m (ml µg^{-1}, ml µg^{-1}, (ml µg^{-1})^2, resp.)	$\kappa_e^m = 0.01462$, $\kappa_d^m = 0.41657$, $\kappa_m^m = 0.0028$
ϵ	rate of point mutations	10^{-4} per locus per cell per division
η	dilution parameter	1% of biomass

were 50× stock solutions in deionized water, sterilized by autoclaving. For M9 minimal medium, they were diluted in water accordingly with 0.2% glucose and 0.1% casamino acid added as nutrients.

The antibiotics used are erythromycin and doxycycline (both Sigma-Aldrich). Liquid stocks were prepared from powder at 50 mg ml^{-1} in ethanol for erythromycin and at 5 mg ml^{-1} in deionized water for doxycycline (afterwards filter sterilized) and frozen at −20°C. All dilutions were prepared in M9 growth medium and stored in the fridge at approximately 5°C.

Batch-transfer experiments were conducted in 96-well microtitre plates with 150 µl liquid volume, each plate was inoculated and transferred using a 96-well replicator. Optical density measurements were taken at 600 nm in a shaken Biotek plate reader.

Data in figure 4b: this illustrates the data produced by one such batch-transfer experiment, here conducted at the drug concentration stated in the figure legend.

Data in figure 5b: preliminary experiments were performed in the same device to determine dose–response relationships for erythromycin and doxycycline, the former is shown in figure 5 (day 1 data). These wells were then transferred to fresh plates for 5 consecutive days.

Data in figure 8b: basal concentrations of both drugs were chosen from the preliminary experiment to achieve

50% inhibition at 24 h ($E_{50} = 9\ \mu g\ ml^{-1}$ for erythromycin and $D_{50} = 0.15\ \mu g\ ml^{-1}$ for doxycycline). Batch transfers we conducted at each of the following combinations:

$$(\theta D_{50},\ (1-\theta)E_{50}) = \left(\frac{0}{15}D_{50},\ \frac{15}{15}E_{50}\right),\ \left(\frac{1}{15}D_{50},\ \frac{14}{15}E_{50}\right),\ ...,$$
$$\left(\frac{15}{15}D_{50},\ \frac{0}{15}E_{50}\right).$$

When $\theta \approx 1/2$, these combination treatments correspond to over 90% inhibition of the bacterial population density relative to a control in which no drug is used [24].

Two controls were included: (i) M9 without antibiotics and without inoculation as a reference for density measurements and (ii) M9 (with glucose) without antibiotics but with inoculation to serve as the uninhibited growth reference. All treatments and controls were replicated 19 times, all plates were pipetted simultaneously.

Each one of the prepared microtitre plates was stored at 4°C until used. To control against drug degradation, a further plate was prepared and stored with the other plates for the duration of the 5-day experiment. At the end of the experiment, this plate was inoculated with an overnight culture of the original colony and measured for 24 h. Both on day 1 and when using this control plate, doxycycline and erythromycin caused a reduction of the AUC with no observed significant differences between these plates. This is consistent with maintenance of the efficacy of the drugs while in cold storage.

Appendix B. Optical density versus live cell counts

In order to demonstrate that measuring optical density at 600 nm in our shaken plate reading devices corresponds to counting live cells densities, we refer to the electronic supplementary material, figure S23, of [24]. This shows a linear correlation between the so-called colony forming units (CFU) and optical density (OD_{600}).

CFUs measure bacterial population densities by diluting a large bacterial population grown in liquid medium a number of times until single colonies can be determined when culturing those dilutions on agar plates, whence the name. So, 'bacterial population density' can be measured equivalently in CFUs per millilitre or in units of OD_{600} according to the electronic supplementary material, figure S23, of [24] which shows a linear correlation between both cell density measures.

Appendix C. Model parameters

Tables 1 and 2.

References

1. Levy AB, Marshall B. 2004 Antibacterial resistance worldwide: causes, challenges and responses. *Nat. Med.* **10**, S122–S129. (doi:10.1038/nm1145)
2. Boucher HW, Talbot GH, Bradley JS, Edwards JE, Gilbert D, Rice LB, Scheld M, Spellberg B, Bartlett J. 2009 Bad bugs, no drugs: no ESKAPE! An update from the infectious diseases society of America. *Clin. Infect. Dis.* **48**, 1–12. (doi:10.1086/595011)
3. Clatworthy AE, Pierson E, Hung DT. 2007 Targeting virulence: a new paradigm for antimicrobial therapy. *Nat. Chem. Biol.* **3**, 541–548. (doi:10.1038/nchembio.2007.24)
4. von Gunten V, Reymond JP, Boubaker K, Gerstel E, Eckert P, Lüthi JC, Troillet N. 2009 Antibiotic use: is appropriateness expensive? *J. Hosp. Infect.* **71**, 108–111. (doi:10.1016/j.jhin.2008.10.026)
5. Livermore D. 2004 Can better prescribing turn the tide of resistance? *Nat. Rev. Microbiol.* **2**, 73–78. (doi:10.1038/nrmicro798)
6. Payne DJ. 2008 Microbiology: desperately seeking new antibiotics. *Science* **321**, 1644–1645. (doi:10.1126/science.1164586)
7. Spellberg B, Powers JH, Brass EP, Miller LG, Edwards JE. 2004 Trends in antimicrobial drug development: implications for the future. *Clin. Infect. Dis.* **38**, 1279–1286. (doi:10.1086/420937)
8. Alp E, van der Hoeven JG, Verweij PE, Mouton JW, Voss A. 2005 Duration of antibiotic treatment: are even numbers odd? *J. Antimicrob. Chemother.* **56**, 441–442. (doi:10.1093/jac/dki213)
9. Roberts JA, Kruger P, Paterson DL, Lipman J. 2008 Antibiotic resistance: what's dosing got to do with it? *Crit. Care Med.* **36**, 2433–2440. (doi:10.1097/CCM.0b013e318180fe62)
10. Pugh R, Grant C, Cooke RPD, Dempsey G. 2011 Short-course versus prolonged-course antibiotic therapy for hospital-acquired pneumonia in critically ill adults. *Cochrane Database Syst. Rev.*, CD007577. (doi:10.1002/14651858.CD007577.pub2)
11. Martinez MN, Papich MG, Drusano GL. 2012 Dosing regimen matters: the importance of early intervention and rapid attainment of the pharmacokinetic/pharmacodynamic target. *Antimicrob. Agents Chemother.* **56**, 2795–2805. (doi:10.1128/AAC.05360-11)
12. Geli P, Laxminarayan R, Dunne M, Smith DL. 2012 'One-size-fits-all'? Optimizing treatment duration for bacterial infections. *PLoS ONE* **7**, e29838. (doi:10.1371/journal.pone.0029838)
13. Taubes G. 2008 The bacteria fight back. *Science* **321**, 356–361. (doi:10.1126/science.321.5887.356)
14. Tabor E. 2008 Bacteria by the book. *Science* **322**, 853–854. (doi:10.1126/science.322.5903.853b)
15. Rice LB. 2008 Bacteria by the book: response. *Science* **322**, 853–854. (doi:10.1126/science.322.5903.853b)
16. Huijben S, Bell AS, Sim DG, Tomasello D, Mideo N, Day T, Read AF. 2013 Aggressive chemotherapy and the selection of drug resistant pathogens. *PLoS Pathog.* **9**, e1003578. (doi:10.1371/journal.ppat.1003578)
17. 1913 Address in pathology on chemotherapeutics. *Lancet* **182**, 445–451. (Originally published as volume 2, issue 4694). (doi:10.1016/S0140-6736(01)38705-6)
18. Dancer SJ. 2004 How antibiotics can make us sick: the less obvious adverse effects of antimicrobial chemotherapy. *Lancet Infect. Dis.* **4**, 611–619. (doi:10.1016/S1473-3099(04)01145-4)
19. Kalghatgi S, Spina CS, Costello JC, Liesa M, Morones-Ramirez JR, Slomovic S, Molina A, Shirihai OS, Collins JJ. 2013 Bactericidal antibiotics induce mitochondrial dysfunction and oxidative damage in mammalian cells. *Sci. Transl. Med.* **5**, 192ra85. (doi:10.1126/scitranslmed.3006055)
20. Sullivan A, Edlund C, Nord CE. 2001 Effect of antimicrobial agents on the ecological balance of human microflora. *Lancet Infect. Dis.* **1**, 101–114. (doi:10.1016/S1473-3099(01)00066-4)
21. Fitzgerald JB, Schoeberl B, Nielsen UB, Sorger PK. 2006 Systems biology and combination therapy in the quest for clinical efficacy. *Nat. Chem. Biol.* **2**, 458–466. (doi:10.1038/nchembio817)
22. Greco WR, Bravo G, Parsons JC. 1995 The search for synergy: a critical review from a response surface perspective. *Pharmacol. Rev.* **47**, 331–385.
23. Read AF, Day T, Huijben S. 2011 The evolution of drug resistance and the curious orthodoxy of aggressive chemotherapy. *Proc Natl Acad. Sci. USA* **108**(Suppl. 2), 10 871–10 877. (doi:10.1073/pnas.1100299108)
24. Pena-Miller R, Laehnemann D, Jansen G, Fuentes-Hernandez A, Rosenstiel P, Schulenburg H, Beardmore R. 2013 When the most potent combination of antibiotics selects for the greatest bacterial load: the smile–frown transition. *PLoS Biol.* **11**, e1001540.

25. Hegreness M, Shoresh N, Damian D, Hartl D, Kishony R . 2008 Accelerated evolution of resistance in multidrug environments. *Proc. Natl Acad. Sci. USA* **105**, 13 977 – 13 981. (doi:10.1073/pnas.0805965105)

26. Yeh PJ, Hegreness MJ, Aiden AP, Kishony R. 2009 Drug interactions and the evolution of antibiotic resistance. *Nat. Rev. Microbiol.* **7**, 460 – 466. (doi:10. 1038/nrmicro2133)

27. Deresinski S. 2009 Vancomycin in combination with other antibiotics for the treatment of serious methicillin-resistant *Staphylococcus aureus* infections. *Clin. Infect. Dis.* **49**, 1072 – 1079. (doi:10. 1086/605572)

28. Bayer AS, Morrison JO. 1984 Disparity between timed-kill and checkerboard methods for determination of *in vitro* bactericidal interactions of vancomycin plus rifampin versus methicillin-susceptible and -resistant *Staphylococcus aureus*. *Antimicrob. Agents Chemother.* **26**, 220 – 223. (doi:10.1128/AAC.26.2.220)

29. Howe RA, Andrews JM. 2012 BSAC standardized disc susceptibility testing method (version 11). *J. Antimicrob. Chemother.* **67**, 2783 – 2784. (doi:10. 1093/jac/dks391)

30. Amsterdam D. 2005 Susceptibility testing of antimicrobials in liquid media. In *Antibiotics in laboratory medicine*, 5th edn (ed. V Lorian), pp. 61 – 143. Philadelphia, PA: Lippincott Williams and Wilkins. (http://books.google.ca/ books?id=HdA4dl8m_T4C\&printsec=front cover\&source=gbs_ge_summary _r\&cad=0\#v=onepage\& q\&f=false).

31. Peña Miller R, Lähnemann D, Schulenburg H, Ackermann M, Beardmore RE. 2012 Selecting against antibioticresistant pathogens: optimal treatments in the presence of commensal bacteria. *Bull. Math. Biol.* **74**, 908 – 934. (doi:10.1007/ s11538-011-9698-5)

32. Peña Miller R, Lähnemann D, Schulenburg H, Ackermann M, Beardmore RE. 2012 The optimal deployment of synergistic antibiotics: a control-theoretic approach. *J. R. Soc. Interface* **9**, 2488 – 2502. (doi:10.1098/rsif.2012.0279)

33. Chou TC, Talalay P. 1981 Generalized equations for the analysis of inhibitions of Michaelis – Menten and higherorder kinetic systems with two or more mutually exclusive and nonexclusive inhibitors. *Eur. J. Biochem.* **115**, 207 – 216. (doi:10.1111/j. 1432-1033.1981.tb06218.x)

34. Andersson DI, Levin BR. 1999 The biological cost of antibiotic resistance. *Curr. Opin. Microbiol.* **2**, 489 – 493. (doi:10.1016/S1369-5274(99)00005-3)

35. Ochman H, Lawrence JG, Groisman Ea. 2000 Lateral gene transfer and the nature of bacterial innovation. *Nature* **405**, 299 – 304. (doi:10.1038/35012500)

36. Weinreich DM, Delaney NF, Depristo MA, Hartl DL. 2006 Darwinian evolution can follow only very few mutational paths to fitter proteins. *Science* **312**, 111 – 114. (doi:10.1126/science.1123539)

37. Sandegren L, Andersson DI. 2009 Bacterial gene amplification: implications for the evolution of antibiotic resistance. *Nat. Rev. Microbiol.* **7**, 578 – 588. (doi:10.1038/nrmicro2174)

38. Wheat PF. 2001 History and development of antimicrobial susceptibility testing methodology. *J. Antimicrob. Chemother.* **48**(Suppl. 1), 1 – 4. (doi:10.1093/jac/48.suppl_1.1)

39. Kahlmeter G *et al*. 2006 European committee on antimicrobial susceptibility testing (EUCAST) technical notes on antimicrobial susceptibility testing. *Clin. Microbiol. Infect.* **12**, 501 – 503. (doi:10.1111/j.1469-0691.2006.01454.x)

40. Eagle H, Musselman AD. 1948 The rate of bactericidal action of penicillin *in vitro* as a function of its concentration, and its paradoxically reduced activity at high concentrations against certain organisms. *J. Exp. Med.* **88**, 99 – 131. (doi:10.1084/ jem.88.1.99)

41. Odds FC. 2003 Synergy, antagonism, and what the chequerboard puts between them. *J. Antimicrob. Chemother.* **52**, 1. (doi:10.1093/jac/dkg301)

42. WHO Library Cataloguing-in-Publication Data: Treatment of tuberculosis: guidelines, 4th edn; 2012 See http://whqlibdoc.who.int/publications/2010/ 9789241547833/_eng.pdf. (accessed 5 April 2012).

43. Kim YS *et al*. 2011 Randomised clinical trial: the efficacy of a 10-day sequential therapy vs. a 14-day standard proton pump inhibitor-based triple therapy for *Helicobacter pylori* in Korea. *Aliment. Pharmacol. Ther.* **34**, 1098 – 1105. (doi:10.1111/j. 1365-2036.2011.04843.x)

44. Vaira D, Zullo A, Hassan C, Fiorini G, Vakil N. 2009 Sequential therapy for *Helicobacter pylori* eradication: the time is now! *Therap. Adv. Gastroenterol.* **2**, 317 – 322. (doi:10.1177/ 1756283X09343326)

45. Greenberg ER *et al*. 2011 14-day triple, 5-day concomitant, and 10-day sequential therapies for *Helicobacter pylori* infection in seven Latin American sites: a randomised trial. *Lancet* **378**, 507 – 514. (doi:10.1016/S0140-6736(11)60825-8)

46. Bergeron M, Ouellette M. 1998 Preventing antibiotic resistance through rapid genotypic identification of bacteria and of their antibiotic resistance genes in the clinical microbiology laboratory. *Clin. Microbiol.* **36**, 2169 – 2172.

47. Bergeron MG, Ouellette M. 1998 Preventing antibiotic resistance using rapid DNA-based diagnostic tests-based diagnostic tests. *Infect. Control Hosp. Epidemiol.* **19**, 560 – 564. (doi:10.2307/30141780)

48. MacDougall C, Polk RE. 2005 Antimicrobial stewardship programs in health care systems. *Clin. Microbiol. Rev.* **18**, 638 – 656. (doi:10.1128/CMR.18. 4.638-656.2005)